PAPER

Nonlinear optical effects in a nucleus

IOP Publishing Journal of Physics G: Nuclear and Particle Physics
J. Phys. G: Nucl. Part. Phys. **48** (2021) 095105 (11pp) https://doi.org/10.1088/1361-6471/ac1712

Nonlinear optical effects in a nucleus

Tao Li[1] **and Xu Wang**[2,*]

[1] Beijing Computational Science Research Center, Beijing 100193, People's Republic of China
[2] Graduate School, China Academy of Engineering Physics, Beijing 100193, People's Republic of China

E-mail: xwang@gscaep.ac.cn

Received 5 April 2021, revised 25 June 2021
Accepted for publication 22 July 2021
Published 19 August 2021

Abstract

Intense laser technologies generate light with unprecedented and growing intensities. The possibility emerges that a nucleus responds nonlinearly to an intense light field, pointing to an emerging research area of nuclear nonlinear optics. Here we consider two-photon and three-photon absorption (with subsequent disintegration) processes of the deuteron, the simplest and the most fundamental nontrivial nucleus, as prototypes of nuclear nonlinear optical effects. Novel observable effects are predicted. Two-photon and three-photon absorptions are shown to lead to remarkably different angular distributions compared to one-photon absorption. Absorption rates are calculated supporting the feasibility of near-future experimental realization. This work paves a way to the emerging field of nuclear nonlinear optics.

Keywords: nonlinear optical effect, ultra-intense laser, multiphoton absorption

(Some figures may appear in colour only in the online journal)

1. Introduction

It is well known that atoms or molecules may respond nonlinearly to a light field if the latter is sufficiently intense. This nonlinear response leads to a host of interesting phenomena, the study of which constitutes the research discipline of nonlinear optics. The first nonlinear optical effect can be dated back to the early 1930s to the prediction of Göppert-Mayer on two-photon absorption of atoms [1], although nonlinear optics flourishes after the invention of lasers in the 1960s. The goal of the current paper is to predict nonlinear optical effects, specifically two-photon and three-photon absorptions, *in a nucleus*.

The reader might ask whether it is timely to consider such nuclear nonlinear optical effects. The answer is yes if one is aware of recent advancements in intense laser technologies. Current

*Author to whom any correspondence should be addressed.

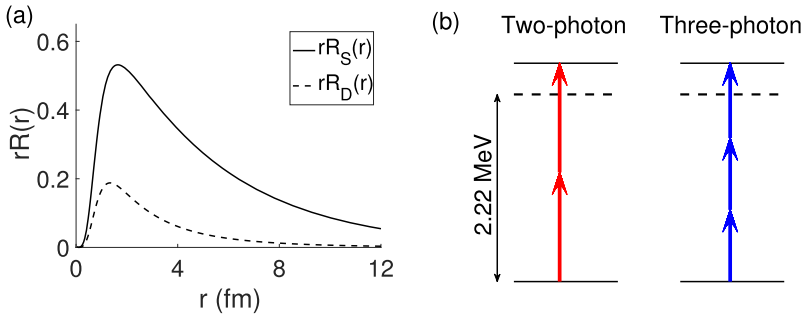

Figure 1. (a) Radial wavefunctions of the deuteron ground state, which consists of an S-component and a D-component. r is the distance between the proton and the neutron. (b) Schematic illustration of two-photon and three-photon absorption processes of the deuteron. 2.22 MeV is the threshold energy of dissociation.

intense laser facilities can generate light (usually in the near infrared) with peak intensities on the order of 10^{22} W cm^{-2}. Enhancements for another one to two orders of magnitude are expected with the next-generation intense laser facilities, for example the extreme light infrastructure of Europe [2–4] or the superintense ultrafast laser facility of Shanghai [5–7]. Ultraintense γ rays can be generated if the above near-infrared laser light interacts with solid targets through highly nonlinear Compton scattering processes [8–12]. The energy conversion from near-infrared laser to γ rays is quite efficient (with energy efficiencies as high as 35%), and γ rays of intensities on the order of 10^{22} W cm^{-2} and durations on the order of 10 fs can be expected in the near future [9].

What will happen if such intense γ rays interact with matter, especially nuclei? Although light-nucleus interaction is an important topic in traditional nuclear physics, extensively studied in processes like γ decay, photoexcitation, photodisintegration, etc, the intensity of the light considered had been rather weak. Will new phenomena emerge if the light becomes very intense? More specifically, will nuclei respond nonlinearly to intense light fields like atoms or molecules do?

In this paper we present answers to the above questions. To enter this new field of nuclear nonlinear optics, it is sensible to start from the simplest instance. We consider the interaction between intense light and the simplest nontrivial nucleus, the deuteron, the role of which in nuclear physics is similar to that of the hydrogen atom in atomic physics. Also we consider the simplest and perhaps the most fundamental nonlinear optical effect, two-photon absorption. (Results for three-photon absorption will also be presented.) The expectation is to construct a foundational model for nuclear nonlinear optics from which physical insights can be gained, and more complex models (with more complex nuclei and/or on more complex nonlinear optical effects) can be constructed.

2. The deuteron and its ground state

For the readers who are not familiar with the deuteron, let us first give a brief description to it. The deuteron consists of a proton (p) and a neutron (n). Using quantum chromodynamics to describe the strong interactions between p and n is extremely demanding, so the p–n potential is usually described phenomenologically. Highly precise effective potentials with different levels of sophistication have been developed [13–16]. The p–n potential is not exactly a central one,

and different angular momenta can be coupled by tensor components of the potential. The deuteron is known to have only one bound state (the ground state) of energy −2.22 MeV. The ground state is a superposition of an S-state (with an angular momentum quantum number $L = 0$) and a D-state ($L = 2$), although the latter is much weaker than the former. The ground state wavefunction can be written as

$$\langle \vec{r}|\psi_i\rangle = R_{\rm S}(r)\mathcal{Y}^{J=1,m_J=1}_{L=0,S=1}(\theta,\phi) + R_{\rm D}(r)\mathcal{Y}^{J=1,m_J=1}_{L=2,S=1}(\theta,\phi), \tag{1}$$

where $\vec{r} = \vec{r}_{\rm p} - \vec{r}_{\rm n}$ is the relative position of the proton with respect to the neutron. $\mathcal{Y}^{J,m_J}_{L,S}(\theta,\phi)$ are eigenstates of the total angular momentum. L, S, J, and m_J are the quantum numbers of the orbital angular momentum, total spin, total angular momentum, and the z-component of the total angular momentum, respectively. The values of these quantum numbers as shown in equation (1) are identified experimentally. The radial wavefunctions of the two components, noted $R_{\rm S}(r)$ and $R_{\rm D}(r)$, are shown in figure 1(a), numerically calculated using the potential of Reid [13]. Note that the wavefunctions are normalized by the condition $\int_0^\infty (R_{\rm S}^2 + R_{\rm D}^2)r^2\,{\rm d}r = 1$.

Because there are no bound excited states, photon absorption brings the deuteron from the ground state to continuum states. Therefore the deuteron will disintegrate (dissociate) subsequently. If the photon energy is higher than the dissociation threshold of 2.22 MeV, the process of one-photon absorption has been studied extensively in nuclear physics [17, 18]. If the photon energy is lower than the threshold, then simultaneous absorption of the energy of more than one photon is required, as illustrated in figure 1(b) for two-photon and three-photon cases. These few-photon absorption processes are the result of nonlinear responses of the deuteron to the external light, and they only happen when the light is very intense. For two-photon absorption, the photon energy considered is within the range of (1.11, 2.22) MeV. If the photon energy is higher than the threshold, two-photon absorption is still possible, but it will be overwhelmed by the more probable one-photon absorption. For three-photon absorption, the considered photon energy is within the range of (0.74, 1.11) MeV. For simplicity, a monochromatic light source is assumed in our calculation, so the absorbed photons have equal energy.

3. Angular distributions of two-photon and three-photon absorption

We aim at making quantitative predictions on two-photon and three-photon absorption processes. One might use the perturbation theory to calculate the light-induced response of the deuteron. However, the perturbation theory is not very convenient for the deuteron system because it involves summing over many (in principle infinite) intermediate continuum states and calculating free-free transition matrix elements, which are known to be nontrivial to deal with. Instead we use a method that avoids these difficulties. The method is called the strong field approximation (SFA), or the Keldysh–Faisal–Reiss (KFR) theory [19–21]. It has been extremely successful in describing highly nonlinear responses of atoms to intense laser fields. These nonlinear responses have led to novel phenomena as multiphoton ionization [23–25], high harmonic generation [26, 27], attosecond pulse generation [28–31], etc. The main idea of SFA is to approximate the continuum states by Volkov states [22], the quantum states of a free charged particle in an external electromagnetic field. This is of course more justified for a short-range potential (which is the case for the deuteron) than for the Coulomb potential (which is the case for atomic ionization). Therefore the SFA method is actually more suitable to deuteron photodisintegration than to atomic ionization, for which the SFA method was originally developed. Details of the SFA method have been documented in references [19–21, 32] and will not be repeated here, but the framework and the main formulas are given in appendix A for the general readers who may not be familiar with this method.

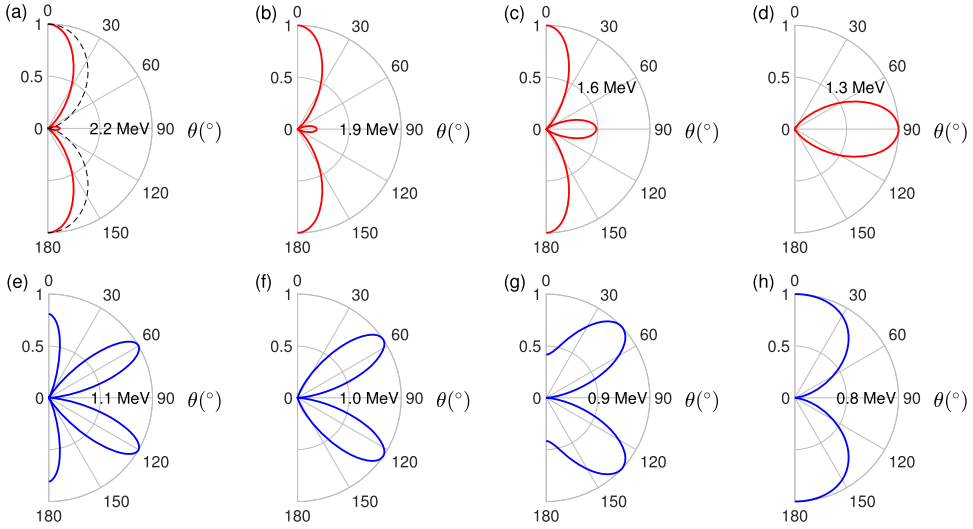

Figure 2. Angular distributions of the proton (or equivalently of the neutron) after two-photon (top row) or three-photon (bottom row) absorption and disintegration of the deuteron. The results are obtained using equations (A.13) and (A.14) in appendix. The corresponding photon energy for each case is labeled on figure (the threshold energy of disintegration is 2.22 MeV). The light is assumed to be linearly polarized along the z axis and the angle θ shown in each figure is the polar angle with respect to the $+z$ direction. Each distribution is normalized to its own peak value. The radial axis is in arbitrary units. The dashed curve in (a) is the dipole shape ($\cos^2\theta$) for one-photon disintegration, which is insensitive to the photon energy and is plotted for the purpose of visual comparison.

First we show that two-photon and three-photon absorptions lead to drastically different observable effects compared to one-photon absorption. For photodisintegration of the deuteron, the angular distribution of the resultant proton (or equivalently of the neutron) is the most informative physical observable. It is known that for one-photon disintegration, a process quite similar to atomic photoionization, the angular distribution is mostly of a dipole (i.e. $\cos^2\theta$) shape and is insensitive to the photon energy [17, 18]. Here we have assumed that the light is linearly polarized along the z axis and θ is the polar angle with respect to the $+z$ direction. Results for two-photon and three-photon absorptions, however, show very different angular distributions with much richer shapes. For example, the top row of figure 2 shows angular distributions of two-photon absorption with four different photon energies. For 2.2 MeV, an energy just below the threshold, the distribution is mostly along 0° and 180°, with however a small lobe along 90°. The difference between this shape and the normal dipole shape of one-photon absorption (dashed curve on the same figure) can be clearly seen. The small lobe along the perpendicular direction grows as the photon energy decreases, as can be seen from the angular distributions for 1.9, 1.6, and 1.3 MeV. For the last case, almost all population is along the perpendicular direction, with virtually none along the polarization direction. One sees from these examples that angular distributions for two-photon absorption depend very sensitively on the photon energy, in contrast to one-photon absorption.

Even more striking photon-energy dependency can be seen from three-photon absorption. The bottom row of figure 2 shows examples of four different photon energies. For 1.1 MeV, the angular distribution has four peaks (lobes) at 0°, 60°, 120°, and 180°. If the photon energy decreases slightly to 1.0 MeV, the distribution changes into two peaks at 55° and 125°, with

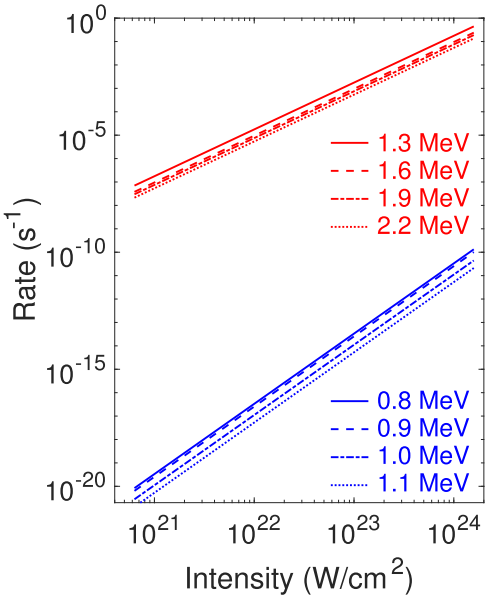

Figure 3. Integrated two-photon (upper lines) and three-photon (lower lines) absorption rates as a function of light intensity. Four different photon energies are used for each category, as labeled. The light is linearly polarized. Note that two-photon rates depend quadratically on the intensity, and three-photon rates depend cubically on the intensity.

virtually no population along the polarization axis. For photon energy 0.9 MeV, the positions of the two peaks shift to 47° and 133°, and the population along the polarization axis increases. If the photon energy deceases to 0.8 MeV, then the population along the polarization axis dominates, with an apparently wider distribution than the dipole shape.

The sensitive photon-energy dependency of two-photon and three-photon absorptions is the result of the competition between the two terms (the one with $\vec{A}\cdot\vec{p}$ and the one with A^2) in the interaction Hamiltonian

$$V_{\rm L} = -\frac{q}{\mu}\vec{A}(t)\cdot\vec{p} + \frac{q^2A^2(t)}{2\mu}, \tag{2}$$

where $q = e/2$ is an effective charge for relative motion and $\vec{A}(t)$ is the vector potential. For linear polarization we use $\vec{A}(t) = \hat{z}A_0\cos\omega t$, then $\vec{A}(t)\cdot\vec{p} = A_0 p\cos\theta\cos\omega t$ and $A^2(t) = A_0^2\cos^2\omega t$. The former term has a polar angle dependency of $\cos\theta$ whereas the latter term does not. Both terms, however, contribute to two-photon and three-photon absorptions with relative weights depending on the photon energy. This is the underlying reason for the photon-energy-sensitive angular distributions shown in figure 2. In contrast, one-photon absorption only involves the $\vec{A}\cdot\vec{p}$ term (because the A^2 term changes the energy by 2ω), and the angular distribution has a rather boring dipole shape insensitive to the photon energy.

4. The absorption rates

Figure 3 shows total two-photon and three-photon absorption rates as a function of light intensity. The rates are integrated values over solid angles. For each category results of four photon

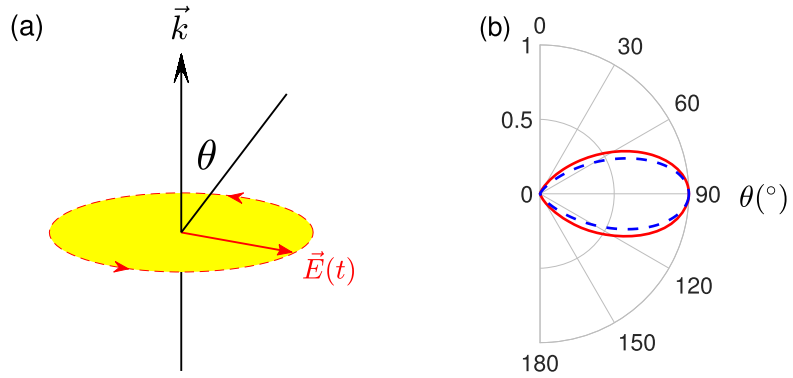

Figure 4. (a) Illustration of convention for circular polarization. The quantization axis is chosen to be the laser propagation axis, and the polar angle θ is with respect to the direction of $\vec{k}$. The laser electric field $\vec{E}(t)$ is perpendicular to and rotates about the propagation axis. (b) Angular distributions for two-photon (red solid curve) and three-photon (blue dashed curve) absorptions. They do not depend on the photon energy.

energies (same as used in figure 2) have been shown, as labeled on figure. One sees that within each category, the absorption rate does not depend very sensitively on the photon energy, although a higher photon energy does lead to slightly lower rates. This is interesting considering the extremely sensitive photon-energy dependency of the angular distributions shown in figure 2.

For the two-photon case the absorption rates can reach about 10^{-5} s^{-1} with intensity 10^{22} W cm^{-2}. Consider the amount of deuterium to be several milligrams, available for example in a deuterium–tritium fuel cell, and a light pulse with duration 10 fs. Then the number of protons (neutrons) generated from two-photon disintegration processes would be on the order of 100 from a single shot. This will open to experimental realization in the near future. Being more optimistic and looking a little further into the future, the two-photon disintegration rate can reach 10^{-1} s^{-1} with intensity 10^{24} W cm^{-2}, and the number of protons (neutrons) generated under the mentioned conditions would be 10^6 per shot.

The three-photon absorption rates are much lower than the two-photon rates. At intensity 10^{21} W cm^{-2}, the difference is about 13 orders of magnitude. The difference shrinks as the intensity increases because of the different slopes of the lines. As would be expected, two-photon rates depend quadratically on the intensity, and three-photon rates depend cubically on the intensity.

5. Results for circular polarization

In the case of circular polarization, the quantization axis is chosen to be the laser propagation axis by convention, and the polar angle θ is with respect to the direction of $\vec{k}$, as illustrated in figure 4(a). The angular distributions have rather simple shapes. For the two-photon case, the angular distribution has a shape of $\sin^4\theta$, independent of the photon energy. The same is true for the three-photon case, except that the shape of the angular distribution becomes $\sin^6\theta$. For circular polarization the A^2 term of the interaction Hamiltonian (equation (2)) does not have a time dependency, and only the $\vec{A}\cdot\vec{p}$ contributes to the dissociation. This leads to the relatively simple angular distributions. The integrated two-photon and three-photon absorption rates are similar to the corresponding cases for linear polarization (figure 3) and will not be shown.

6. Conclusions

We consider two-photon and three-photon absorptions of the deuteron as the simplest scenario of nuclear nonlinear optics. The possibility of nonlinear optical effects in nuclei is driven by rapid advancements of intense laser technologies. Indeed, one sees increasing attention and research efforts on light-nucleus interactions during the past few years. For example, the interaction between Mössbauer ^{57}Fe nuclei and 14.4 keV photons from synchrotron radiations has been used to demonstrate collective nuclear quantum optical effects [33–40]. Analyses have also been made on the possibility of using intense light to influence α decay [41–43], nuclear fission [44], or nuclear fusion [45–47] processes.

We have performed calculations on the two-photon and three-photon absorption processes of the deuteron. The absorption of photons will be accompanied by subsequent dissociation of the deuteron, leaving informative and observable effects in the angular distribution of the resultant proton (neutron). Two-photon and three-photon angular distributions show rich shapes and sensitive energy dependency, in remarkable contrast to one-photon angular distributions. Besides the angular distributions, we have also calculated the integrated absorption rates. The two-photon rates are high enough for upcoming experimental testings.

Extension to more complex nuclei and to other nonlinear optical effects can be anticipated. Intense light-nuclei interaction would supply new ways or methods to control nuclei, as well as new ways to change the property of the light in regimes inaccessible to normal optics. There is certainly much to be expected in the emerging field of nuclear nonlinear optics.

Acknowledgments

The authors thank Professor Chang-Pu Sun for reading the manuscript and providing helpful suggestions. This work is supported by Science Challenge Project of China No. TZ2018005, NSFC No. 11774323, No. 12088101, and NSAF No. U1930403.

Data availability statement

All data that support the findings of this study are included within the article (and any supplementary files).

Appendix A. The SFA method

Here we outline the theoretical framework and the main formulas of the method that we use in the main text. The method is called the SFA, or the KFR theory by the names of the developers.

The total Hamiltonian of the deuteron in an electromagnetic field can be separated into a center-of-mass part and a relative-motion part. Since it is the dissociation process that is of interest, we will be focusing on the latter part, which has the following terms

$$H = \frac{\hat{p}^2}{2\mu} + V_{\rm pn} + V_{\rm L}, \tag{A.1}$$

where $\hat{p}$ is the momentum operator for the relative motion, $\mu = M/2$ is the reduced mass with M the mass of the proton (also approximately of the neutron), $V_{\rm pn}$ is the (phenomenological) p–n potential, and $V_{\rm L}$ is the interaction potential with the external light field. For convenience

let us also define

$$H_0 = \frac{\hat{p}^2}{2\mu} + V_{\rm pn}; \tag{A.2}$$

$$H_{\rm L} = \frac{\hat{p}^2}{2\mu} + V_{\rm L}, \tag{A.3}$$

both being part of the total (relative-motion) Hamiltonian H.

In the velocity gauge [21, 48, 49], the interaction potential $V_{\rm L}$ is given as

$$V_{\rm L} = -\frac{q}{\mu}\vec{A}(t)\cdot\hat{p} + \frac{q^2A^2(t)}{2\mu}, \tag{A.4}$$

where $q = e/2$ is the effective charge in relative motion and $\vec{A}(t)$ is the vector potential. Since the light considered here is very intense, the A^2 term in the interaction cannot be neglected as for weak light fields. As we show in the main text, this term plays an important role in the angular distributions of two-photon and three-photon absorptions. We are mainly interested in light with photon energies below the dissociation threshold (2.22 MeV), or the wavelengths being longer than about 550 fm, which is much larger than the size of the deuteron itself ($\approx$1 fm). The spatial variation of the vector potential can therefore be neglected. Here we choose $\vec{A}(t) = \vec{\epsilon}A_0\cos\omega t$, where the vector potential has been assumed to have a sinusoidal form linearly polarized along direction $\vec{\epsilon}$.

If at time t_0 the deuteron is in its ground state $|\psi_i\rangle$, then the probability amplitude of finding the system later in a final plane-wave state $|\psi_{\vec{p}}\rangle$ is

$$M_{\vec{p}}(t,t_0) = \langle\psi_{\vec{p}}|U(t,t_0)|\psi_i\rangle, \tag{A.5}$$

with $\langle\vec{r}|\psi_{\vec{p}}\rangle = (2\pi)^{-3/2}\,{\rm e}^{{\rm i}\vec{p}\cdot\vec{r}}$. $U(t,t_0)$ is the time-evolution operator corresponding to the total Hamiltonian H. Because of the complexity of $V_{\rm pn}$, there is no simple analytical form for $U(t,t_0)$. However, the time-evolution operators corresponding to the Hamiltonian H_0 and $H_{\rm L}$ are much simpler with the following forms

$$U_0(t,t_0)|\psi_i\rangle = \exp\left\{-{\rm i}E_i(t-t_0)\right\}|\psi_i\rangle; \tag{A.6}$$

$$\begin{aligned} U_{\rm L}(t,t_0)|\psi_{\vec{p}}\rangle = \exp\Bigg\{&-{\rm i}\left(\frac{p^2}{2\mu}+\eta\omega\right)(t-t_0) + {\rm i}\sqrt{\eta\alpha}(\sin\omega t - \sin\omega t_0) \\ &- \frac{{\rm i}\eta}{2}(\sin 2\omega t - \sin 2\omega t_0)\Bigg\}|\psi_{\vec{p}}\rangle. \end{aligned} \tag{A.7}$$

In equation (A.6) E_i is the energy of the ground state. In equation (A.7) we have used equations (A.3) and (A.4) and defined for convenience $\eta \equiv q^2A_0^2/4\mu\omega$ and $\alpha \equiv 4(\vec{\epsilon}\cdot\vec{p})^2/\mu\omega$. It is to be pointed out that $\eta\omega$ is the ponderomotive energy of the proton. For example, for the deuteron in a light field with intensity 10^{24} W cm^{-2} and photon energy 0.8 MeV, $\eta \sim 10^{-10} \ll 1$. The relationship $\eta \ll 1$ holds for all the results reported in this paper. This means that the ponderomotive energy is much smaller than the photon energy.

It can be proved that U and U_0 are related by the following equation

$$U(t,t_0) = U_0(t,t_0) - {\rm i}\int_{t_0}^{t} U(t,t_1)V_{\rm L}(t_1)U_0(t_1,t_0){\rm d}t_1. \tag{A.8}$$

If the propagator U inside the integral of equation (A.8) is approximated by $U_{\rm L}$, then the transition amplitude $M_{\vec{p}}$ in equation (A.5) can be written as

$$M_{\vec{p}}(t,t_0) \approx -\mathrm{i}\int_{t_0}^{t} \langle\psi_{\vec{p}}|U_{\rm L}(t,t_1)V_{\rm L}(t_1)U_0(t_1,t_0)|\psi_i\rangle \mathrm{d}t_1. \tag{A.9}$$

This approximation is called the SFA, developed by Keldysh [19], Faisal [20], and Reiss [21]. The SFA transition amplitude has a clear physical picture: the system starts from the initial state $|\psi_i\rangle$ at t_0, propagates under the influence of H_0 until time t_1, when it is kicked by the laser potential $V_{\rm L}$, and from t_1 to t the system propagates under the influence of $H_{\rm L}$, neglecting the effect of the the p–n binding potential. SFA has been widely used to describe the interaction between atoms and intense laser fields. In fact, as explained in the main text, SFA is more suitable for the deuteron system because the p–n potential is of short range, and neglecting the binding potential in the continuum state is more justified than for atoms with long-range Coulomb potentials.

We continue by substituting equations (A.4), (A.6) and (A.7) into equation (A.9). The following expansion will be used [21]

$$\exp\left\{\frac{\mathrm{i}\eta}{2}\sin 2\omega t - \mathrm{i}\sqrt{\eta\alpha}\sin\omega t\right\} \approx \sum_{n=-\infty}^{\infty}\left(-\frac{\eta}{4}\right)^{n/2}\zeta_n(\alpha)\mathrm{e}^{-\mathrm{i}n\omega t}, \tag{A.10}$$

for $\eta \ll 1$. Here $\zeta_n(\alpha) \equiv \sum_k (-\alpha)^k/(2k)!(n/2-k)!$, and n takes integer values. For even n, $k = 0, 1, \ldots, n/2$; and for odd n, $k = 1/2, 3/2, \ldots, n/2$. The transition amplitude can then be written in the following concise form in the long-time limit (i.e. for pulses much longer than an optical period)

$$M_{\vec{p}}(t\to\infty, t_0\to-\infty) \approx \mathrm{i}\frac{\tilde{\psi}_i(\vec{p})}{\sqrt{2\pi}}\sum_n n\omega\left(-\frac{\eta}{4}\right)^{n/2}\zeta_n(\alpha)\delta\left(\frac{p^2}{2\mu} - E_i - n\omega\right), \tag{A.11}$$

where $\tilde{\psi}_i(\vec{p}) = (2\pi)^{3/2}\langle\psi_{\vec{p}}|\psi_i\rangle$ is the momentum component of the deuteron ground state, or the Fourier transformation of equation (1). The transition amplitude is a summation over different disintegration channels, distinguished by the number of photons absorbed. For a channel with n absorbed photons, the delta function imposes the energy conservation condition.

The differential rates (angular distributions) can be obtained by integrating out the final $\vec{p}$ in each solid angle

$$\frac{\mathrm{d}w}{\mathrm{d}\Omega} = \int p^2\,\mathrm{d}p \lim_{\substack{t_0\to-\infty\\ t\to\infty}} \frac{|M_{\vec{p}}(t,t_0)|^2}{t-t_0} = \frac{\sqrt{2\mu^3\omega^5}}{4\pi^2}\sum_{n=n_0}^{\infty} n^2\sqrt{n+\frac{E_i}{\omega}}\left(\frac{\eta}{4}\right)^n |\tilde{\psi}_i(\vec{p}_n)|^2\zeta_n^2(\alpha_n), \tag{A.12}$$

where n_0 is the minimum number of photons required for dissociation (the integer just greater than $-E_i/\omega$) and $p_n = \sqrt{2\mu(E_i+n\omega)}$ fulfilling the delta-function energy constraint in equation (A.11). The total disintegration rate w can be obtained by integrating the differential rates over all solid angles.

As mentioned earlier the condition $\eta \ll 1$ holds in our calculation, and equation (A.12) is a sum of η^n, only the n_0 term needs to be kept (that is, 'above-threshold' disintegrations can be neglected). $n_0 = 1$ corresponds to single-photon disintegration which has been studied in traditional nuclear physics. $n_0 > 1$ corresponds to the cases that multiple photons need to be absorbed simultaneously to disintegrate the deuteron. Then the angular distribution

equation (A.12) can be simplified to

$$\frac{\mathrm{d}w}{\mathrm{d}\Omega} \approx \frac{\sqrt{2\mu^3\omega^5}}{4\pi^2} n_0^2 \sqrt{n_0 + \frac{E_i}{\omega}} \left(\frac{\eta}{4}\right)^{n_0} |\tilde{\psi}_i(\vec{p}_{n_0})|^2 \times \sum_{k=0}^{n_0/2} \sum_{l=0}^{n_0/2} \frac{(-8)^{k+l}\left(n_0 + \frac{E_i}{\omega}\right)^{k+l} (\cos\,\theta)^{2k+2l}}{(2k)!\,(2l)!\,\left(\frac{n_0}{2}-k\right)!\,\left(\frac{n_0}{2}-l\right)!} \tag{A.13}$$

for even n_0, and

$$\frac{\mathrm{d}w}{\mathrm{d}\Omega} \approx \frac{2\sqrt{2\mu^3\omega^5}}{\pi^2} n_0^2 \left(n_0 + \frac{E_i}{\omega}\right)^{\frac{3}{2}} \left(\frac{\eta}{4}\right)^{n_0} |\tilde{\psi}_i(\vec{p}_{n_0})|^2 \times \sum_{k=0}^{\frac{n_0-1}{2}} \sum_{l=0}^{\frac{n_0-1}{2}} \frac{(-8)^{k+l}\left(n_0 + \frac{E_i}{\omega}\right)^{k+l} (\cos\,\theta)^{2k+2l+2}}{(2k+1)!\,(2l+1)!\,\left(\frac{n_0-1}{2}-k\right)!\,\left(\frac{n_0-1}{2}-l\right)!} \tag{A.14}$$

for odd n_0. Here θ is the polar angle with respect to $\vec{\epsilon}$, the direction of the laser vector potential.

It is easy to find that the kinetic energy of the center of mass $p_{\mathrm{cm}} \sim A_0^2/M$ is less than the photon energy ω by more than 10 orders of magnitude. Therefore the motion of the center of mass can be neglected. The kinetic energy of the emitted proton is less than the photon energy ω (neglecting above-threshold disintegrations). The momentum of the proton is therefore less than $\sqrt{2\mu\omega}$. With this condition the D-component of the deuteron ground state, constituting a few percent in population, contributes little to the disintegration. This is because the S-component has more low-momentum fractions than the D-component does. We have checked that the relative contribution from the D-component is less than 10^{-3} in the disintegration process.

For circularly polarized light, the vector potential can be written as

$$\vec{A}(t) = \frac{A_0}{2}\left(\vec{\epsilon}\,\mathrm{e}^{\mathrm{i}\omega t} + \vec{\epsilon}^{\,*}\,\mathrm{e}^{-\mathrm{i}\omega t}\right), \tag{A.15}$$

where $\vec{\epsilon}\cdot\vec{\epsilon} = 0$, $\vec{\epsilon}\cdot\vec{\epsilon}^{\,*} = 1$. The differential disintegration rate reads

$$\frac{\mathrm{d}w}{\mathrm{d}\Omega} \approx \frac{\sqrt{2\mu^3\omega^5}}{4\pi^2} \frac{\left(n_0 + \frac{E_i}{\omega}\right)^{n_0+\frac{1}{2}}}{[(n_0-1)!]^2} |\tilde{\psi}_i(\vec{p}_{n_0})|^2 \eta^{n_0} (\sin\,\theta)^{2n_0}. \tag{A.16}$$

Only the n_0 order is kept. Note that for circular polarization, the polar angle θ is defined with respect to the laser propagation direction. One finds that the differential cross section depends on θ only through the last $(\sin\,\theta)^{2n_0}$ term. That is, for the same n_0, different photon energies lead to the same shape of angular distribution.

ORCID iDs

Tao Li https://orcid.org/0000-0003-0288-4332
Xu Wang https://orcid.org/0000-0002-8043-7135

References

[1] Göppert-Mayer M 1931 *Ann. Phys., Lpz.* **401** 273
[2] Ur C A, Balabanski D, Cata-Danil G, Gales S, Morjan I, Tesileanu O, Ursescu D, Ursu I and Zamfir N V 2015 *Nucl. Instrum. Methods Phys. Res.* B **355** 198

[3] Balabanski D L, Popescu R, Stutman D, Tanaka K A, Tesileanu O, Ur C A, Ursescu D and Zamfir N V 2017 *Europhys. Lett.* **117** 28001
[4] Balabanski D L, Constantin P, Rotaru A and State A 2019 *Hyperfine Interact.* **240** 49
[5] Li W *et al* 2018 *Opt. Lett.* **43** 5681
[6] Yu L *et al* 2018 *Opt. Express* **26** 2625
[7] Zhang Z *et al* 2020 *High Power Laser Sci. Eng.* **8** E4
[8] Cipiccia S *et al* 2011 *Nat. Phys.* **523** 867
[9] Ridgers C P, Brady C S, Duclous R, Kirk J G, Bennett K, Arber T D, Robinson A P L and Bell A R 2012 *Phys. Rev. Lett.* **108** 165006
[10] Sarri G *et al* 2014 *Phys. Rev. Lett.* **113** 224801
[11] Yu C *et al* 2016 *Sci. Rep.* **6** 29518
[12] Chang H X, Qiao B, Huang T W, Xu Z, Zhou C T, Gu Y Q, Yan X Q, Zepf M and He X T 2017 *Sci. Rep.* **7** 45031
[13] Reid R V 1968 *Ann. Phys., NY* **50** 411
[14] Nagels M M, Rijken T A and de Swart J J 1978 *Phys. Rev.* D **17** 768
[15] Lacombe M, Loiseau B, Richard J M, Vinh Mau R, Côté J, Pirès P and de Tourreil R 1980 *Phys. Rev.* C **21** 861
[16] Wiringa R B, Stoks V G J and Schiavilla R 1995 *Phys. Rev.* C **51** 38
[17] Rustgi M L, Zernik W, Breit G and Andrews D J 1960 *Phys. Rev.* **120** 1881
[18] Ying S, Henley E M and Miller G A 1988 *Phys. Rev.* C **38** 1584
[19] Keldysh L V 1965 *Sov. Phys. JETP* **20** 1307
[20] Faisal F H M 1973 *J. Phys. B: At. Mol. Phys.* **6** L89
[21] Reiss H R 1980 *Phys. Rev.* A **22** 1786
[22] Volkov D M 1935 *Z. Phys.* **94** 250
[23] Voronov G and Delone N 1965 *JETP Lett.* **1** 66
[24] Agostini P, Barjot G, Bonnal J, Mainfray G, Manus C and Morellec J 1968 *IEEE J. Quantum Electron.* **4** 667
[25] Agostini P, Fabre F, Mainfray G, Petite G and Rahman N K 1979 *Phys. Rev. Lett.* **42** 1127
[26] McPherson A, Gibson G, Jara H, Johann U, Luk T S, McIntyre I A, Boyer K and Rhodes C K 1987 *J. Opt. Soc. Am.* B **4** 595
[27] Ferray M, L'Huillier A, Li X F, Lompre L A, Mainfray G and Manus C 1988 *J. Phys. B: At. Mol. Opt. Phys.* **21** L31
[28] Krausz F and Ivanov M 2009 *Rev. Mod. Phys.* **81** 163
[29] Zhao K, Zhang Q, Chini M, Wu Y, Wang X and Chang Z 2012 *Opt. Lett.* **37** 3891
[30] Li J *et al* 2017 *Nat. Commun.* **8** 186
[31] Gaumnitz T, Jain A, Pertot Y, Huppert M, Jordan I, Ardana-Lamas F and Wörner H J 2017 *Opt. Express* **25** 27506
[32] Popruzhenko S V 2014 *J. Phys. B: At. Mol. Opt. Phys.* **47** 204001
[33] Röhlsberger R, Schlage K, Sahoo B, Couet S and Rüffer R 2010 *Science* **328** 1248
[34] Röhlsberger R, Wille H-C, Schlage K and Sahoo B 2012 *Nature* **482** 199
[35] Heeg K P *et al* 2013 *Phys. Rev. Lett.* **111** 073601
[36] Heeg K P, Ott C, Schumacher D, Wille H C, Röhlsberger R, Pfeifer T and Evers J 2015 *Phys. Rev. Lett.* **114** 203601
[37] Vagizov F, Antonov V, Radeonychev Y V, Shakhmuratov R N and Kocharovskaya O 2014 *Nature* **508** 80
[38] Haber J, Kong X, Strohm C, Willing S, Gollwitzer J, Bocklage L, Rüffer R, Pálffy A and Röhlsberger R 2017 *Nat. Photon.* **11** 720
[39] Bürvenich T J, Evers J and Keitel C H 2006 *Phys. Rev. Lett.* **96** 142501
[40] Bürvenich T J, Evers J and Keitel C H 2006 *Phys. Rev.* C **74** 044601
[41] Delion D S and Ghinescu S A 2017 *Phys. Rev. Lett.* **119** 202501
[42] Qi J, Li T, Xu R, Fu L and Wang X 2019 *Phys. Rev.* C **99** 044610
[43] Pálffy A and Popruzhenko S V 2020 *Phys. Rev. Lett.* **124** 212505
[44] Qi J, Fu L and Wang X 2020 *Phys. Rev.* C **102** 064629
[45] Queisser F and Schützhold R 2019 *Phys. Rev.* C **100** 041601(R)
[46] Lv W, Duan H and Liu J 2019 *Phys. Rev.* C **100** 064610
[47] Wang X 2020 *Phys. Rev.* C **102** 011601(R)
[48] Yang K-H 1976 *Ann. Phys., NY* **101** 62
[49] Reiss H R 2007 *Phys. Rev.* A **76** 033404